Electronic structure of the double-exchange ferromagnet La$_{0.825}$Sr$_{0.175}$MnO$_3$ studied by optical reflectivity

K. Takenaka,* Y. Sawaki, R. Shiozaki, and S. Sugai

Department of Physics, Nagoya University, Nagoya 464-8602, Japan

(Received 24 July 2000)

Temperature-dependent optical reflectivity spectra were measured on cleaved surfaces of La$_{0.825}$Sr$_{0.175}$MnO$_3$ single crystals up to 6.6 eV. The present result demonstrates that the exchange-gap excitation in the optical conductivity spectrum splits into two parts ($\sim$3.2 and $\sim$5 eV). This indicates that the t_{2g} orbitals also participate in the reconstruction of the optical excitation caused by spin polarization. Based on the present result, we propose and discuss a model for the electronic structure of this prototypical double-exchange material. We also discuss the charge dynamics of the conducting carriers in terms of being a *bad metal*.

Optical spectroscopy is an effective tool for investigating the electrical properties of conducting carriers as well as the electronic structure in the vicinity of the Fermi level (E_F). For doped manganites, which show the intriguing phenomenon of colossal magnetoresistance,[1] the optical spectrum has frequently been used as an experimental basis to help explain the theories behind it.[2–10] However, the optical spectra, and especially the reflectivity $R(\omega)$ spectra, are rather confused and controversial in the field.[11–17] Recently, we have ascertained that this is because the $R(\omega)$ spectra of the manganites are quite sensitive to the surface condition.[14,17]

We discuss the electronic structure of a doped manganite La$_{0.825}$Sr$_{0.175}$MnO$_3$ (LSMO, T_C=283 K) based on reliable $R(\omega)$ spectra measured on *cleaved* surfaces, which cover the energy range 0.02−6.6 eV at 10−295 K and 0.005−40 eV at 295 K. The present result shows that the exchange-gap excitation in $\sigma(\omega)$ of LSMO splits into two parts ($\sim$3.2 eV and $\sim$5 eV). This indicates that not only the e_g but also the t_{2g} orbitals participate in the reconstruction of the optical excitation, or the transfer of spectral weight in $\sigma(\omega)$, caused by spin polarization in a double-exchange (DE) system. We propose a band diagram for LSMO and also discuss the charge dynamics of the conducting carriers in terms of being a *bad metal*.

Single crystals of LSMO were grown by a floating-zone method.[18] All of the reflectivity spectra were measured on cleaved surfaces, typically 1×1 mm^2, using a Fourier-type interferometer (0.005−1.6 eV), a grating spectrometer (0.8−6.6 eV), and a Seya-Namioka type spectrometer (4.0−40 eV) at Institute for Molecular Science, Okazaki National Research Institutes. The details of the experiments were described in our previous papers.[14,17]

Figure 1 shows the temperature (T) dependent reflectivity spectra of LSMO on a logarithmic R scale. The dashed line represents $R(\omega)$ obtained at 295 K. As T decreases, $R(\omega)$ changes from insulating to metallic behavior; the reflectivity edge at about 1.6 eV becomes sharpened and the optical phonons are screened. In addition, one should note that the present spectra exhibit T dependence up to $\sim$6 eV, which is much larger than that of the other strongly correlated materials, which are at most, $\sim$3 eV.[19]

In order to make more detailed and quantitative discussions, we deduce optical conductivity $\sigma(\omega)$ (Fig. 2) from $R(\omega)$ via a Kramers-Kronig transformation.[17] For the extrapolation at the low-energy part, we assumed a constant R for the insulating phase (T=295 K) and a Hagen-Rubens formula for the metallic phase ($T\leq$278 K). Since variation of the extrapolation procedures had a negligible effect on $\sigma(\omega)$ above $\sim$30 meV, the following arguments are independent of the extrapolation. Above 6.6 eV we assumed that the reflectivity is independent of temperature and the 295-K spectrum (inset of Fig. 1) was used for the spectra at all temperatures, because the T variation of $R(\omega)$ in the range 6−6.6 eV was negligibly small and the connection was smooth. In addition, the integrated spectral weight defined by

$$N_{\text{eff}}^*(\omega) = \frac{2m_0 V}{\pi e^2} \int_0^\omega \sigma(\omega') d\omega' \qquad (1)$$

(m_0 is the bare-electron mass; V is the unit-cell volume) almost converges ($\Delta N_{\text{eff}}^*/N_{\text{eff}}^* \lesssim 1.5\%$) at 6.6 eV (inset of Fig. 2). These facts seem to support our analytical procedure.
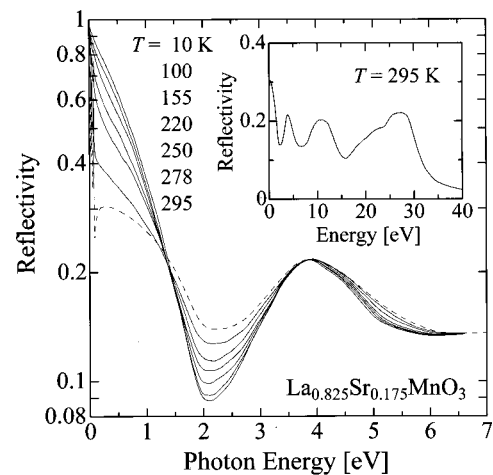

FIG. 1. Temperature-dependent optical reflectivity spectra measured on the cleaved surfaces of La$_{0.825}$Sr$_{0.175}$MnO$_3$. Dashed line represents the data taken at 295 K. Inset: Reflectivity spectrum measured at 295 K up to 40 eV.

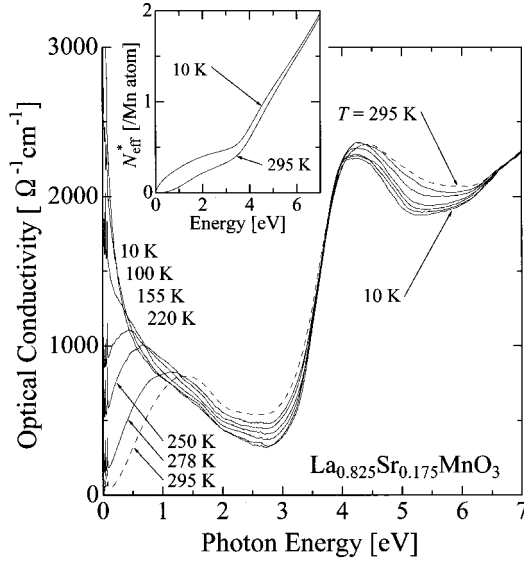FIG. 2. Temperature-dependent optical conductivity spectra of La$_{0.825}$Sr$_{0.175}$MnO$_3$ deduced from the reflectivity spectra via a Kramers-Kronig transformation. Inset: Effective carrier number $N^*_{\text{eff}}(\omega)$ defined as the integration of $\sigma(\omega)$.

With decreasing T, the spectral weight above the reflectivity edge, ~ 1.6 eV, decreases, but the spectral weight below it increases instead. There are two regions in $\sigma(\omega)$, around 3 and 5 eV, where the spectral weight decreases with decreasing T. The spectral weight transfers from the higher-energy regions to a Drude-like ($\omega = 0$ centered) structure as T decreases.

The two energy regions with large T dependence are more clearly shown by the differential conductivity defined by $\Delta\sigma(\omega,T) \equiv \sigma(\omega,T) - \sigma(\omega,10\text{ K})$ [Fig. 3(a)]. The low-energy (less than 2 eV) T dependence in $\Delta\sigma$ is probably induced by both the spectral weight and spectral width of the intraband (or free-carrier) term. Fortunately, this falls off at higher frequencies. Therefore, we conclude that there are *two* higher-lying bands at ~ 3.2 eV and at ~ 5 eV.

The DE model predicts that the spectral weight of the exchange-gap excitation is scaled to $1 - (M/M_S)^2$ [$M(T)$ is the magnetization; M_S is the saturated magnetization] and the missing spectral weight at the higher-lying exchange-gap excitation is transferred to the lower-lying intraband (Drude) excitation as T decreases.[2] The integrated spectral weight of the 3.2-eV and the 5-eV bands in $\Delta\sigma(\omega,T)$, S_{2-4} and S_{4-7}, are estimated by Eq. (1). Here, the suffixes $2-4$ and $4-7$ mean that the integrating energy ranges are $2-4$ eV and $4-7$ eV, respectively. In Fig. 3(b), S_{2-4} and S_{4-7} are found to be proportional to $1-(M/M_S)^2$.[20] Namely, *both the 3.2-eV and the 5-eV bands are the exchange-gap excitations.* Although the higher (5-eV) band has not been clearly observed so far, our result is reasonable in terms of the *f*-sum rule because the lower (3.2-eV) band compensates *only half* of the spectral weight associated with the intraband excitation (inset of Fig. 2). In addition, the optical absorption study also suggests that the spectrum varies with T above 4 eV.[13] The split of the exchange-gap excitation indicates that the t_{2g} orbitals also participate in the reconstruction of the optical excitation caused by spin polarization. The previous treatment of the t_{2g} electrons as the localized spin $s=3/2$ may be oversimplified.
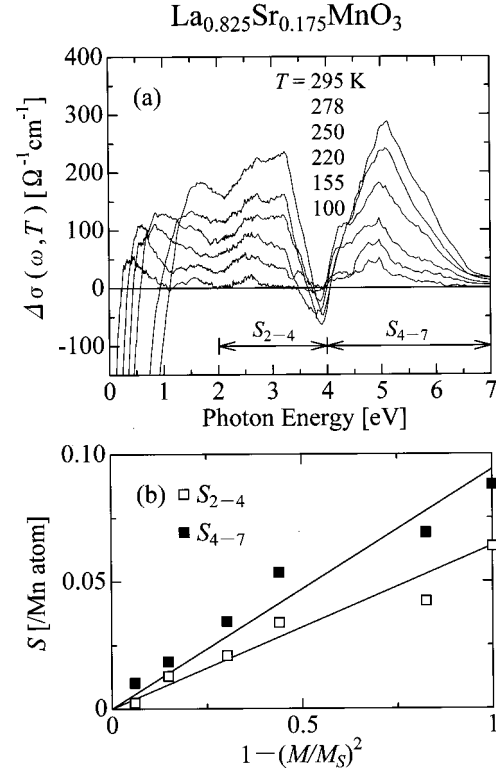
La$_{0.825}$Sr$_{0.175}$MnO$_3$

FIG. 3. (a) Differential conductivity $\Delta\sigma(\omega,T) \equiv \sigma(\omega,T) - \sigma(\omega,10\text{ K})$. (b) Spectral weight of the higher-lying two bands in $\Delta\sigma$, S_{2-4} and S_{4-7}, plotted against $1-(M/M_S)^2$.

The split of the exchange gap enables us to determine the electronic structure less ambiguously (Fig. 4). The two exchange gaps are assigned as follows: the 3.2-eV band, $e_g\uparrow \rightarrow t_{2g}\downarrow$; the 5-eV band, $e_g\uparrow \rightarrow e_g\downarrow$ and $t_{2g}\uparrow \rightarrow t_{2g}\downarrow$. Crystal-field splitting $10Dq$ and exchange splitting sJ_H (here, $s=2$) are estimated to be ~ 1.8 eV and ~ 5 eV, respectively. The estimate of $10Dq$ is roughly coincident with the result of the soft-x-ray absorption study.[21] Previously sJ_H was estimated to be ~ 3 eV, but this is because the 3.2-eV band was assigned as $e_g\uparrow \rightarrow e_g\downarrow$ there.[11,12]
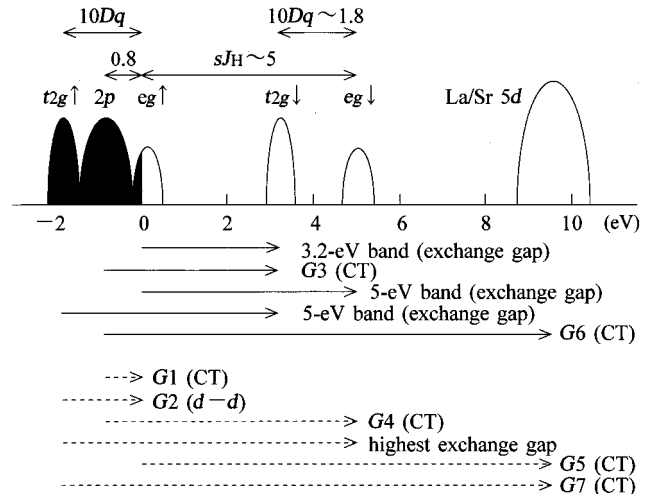

FIG. 4. Schematic band diagram for La$_{0.825}$Sr$_{0.175}$MnO$_3$. Solid area represents occupied states. Solid and dashed arrows represent "obvious" and "hidden" peaks in $\sigma(\omega)$, respectively.
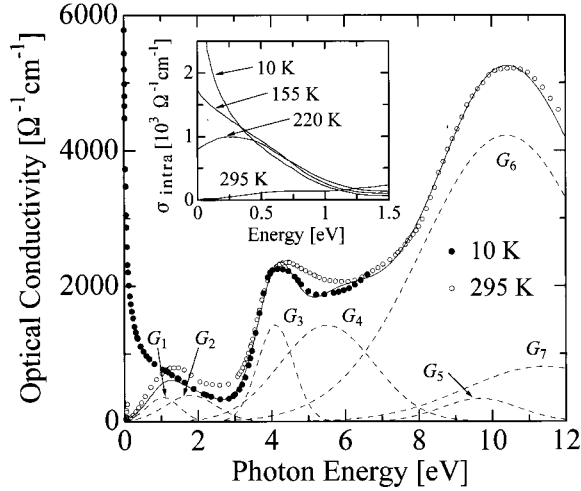
FIG. 5. Result of Gaussian fit. Solid and open circles represent 10-K and 295-K data, respectively. The sum of Gaussians, $\sigma_{\text{inter}}(\omega)$, is represented by a solid line and each $G_i(\omega)$ term by dashed lines. Inset: The intraband conductivity $\sigma_{\text{intra}}(\omega,T) \equiv \sigma(\omega,T) - \sigma_{\text{inter}}(\omega)$. Optical phonons are subtracted.

The peak at ~ 4 eV is independent of T, and hence is considered to be a $2p-3d$ charge-transfer (CT) excitation. The pronounced peak at ~ 10.5 eV (Fig. 5) is also assigned as the CT excitation $2p \rightarrow$ La/Sr $5d$ by other spectroscopic studies.[22,23] Therefore, the 4-eV peak is assigned as $2p \rightarrow t_{2g}\downarrow$, which is the same as that ascribed by Arima and Tokura.[24] Other possible assignments, such as $2p \rightarrow e_g\uparrow$, cannot explain the whole of the spectrum because the La/Sr $5d$ band then becomes too close to E_F. The present spectrum indicates that the energy difference between $2p$ and $e_g\uparrow$ is about 0.8 eV, and hence the $2p$ band is closer to E_F than the $t_{2g}\uparrow$ band. This is consistent with the other optical study.[23]

The above diagram predicts several excitations that are not recognized as peaks in the actual $\sigma(\omega)$ spectrum (dashed arrows in Fig. 4). These ''hidden'' peaks are clues to checking the validity of the proposed diagram. For this purpose, we make the following analyses on $\sigma(\omega)$ at 10 K (solid circles in Fig. 5) over a range $0-12$ eV. [At $6.6-12$ eV we use $\sigma(\omega)$ at 295 K (open circles in Fig. 5).] At 10 K, the contributions to $\sigma(\omega)$ from the exchange-gap excitations are considered to be negligibly small because $M(T)$ almost reaches M_S [M was $\sim 4.0\mu_B$/Mn and nearly T independent at 10 K (Ref. 25)]. Therefore, $\sigma(\omega)$ is formed by the sum of an intraband (Drude-like) term, $\sigma_{\text{intra}}(\omega)$, and an interband term, $\sigma_{\text{inter}}(\omega)$, consisting of the CT and d-d excitations *without* exchange gaps. We assume that $\sigma_{\text{inter}}(\omega)$ is the sum of seven Gaussians $\Sigma_{i=1}^{7} G_i(\omega)$,

$$G_i(\omega) = \frac{S_i}{\gamma_i \sqrt{2\pi}} \exp\left[-\frac{(\omega - \omega_i)^2}{2\gamma_i^2} \right]. \tag{2}$$

Here, S_i, γ_i, and ω_i correspond to spectral weight, damping rate, and peak energy of the ith Gaussian, respectively. The seven Gaussians are assigned as $2p \rightarrow e_g\uparrow$ ($G_1, \sim 0.8$ eV), $t_{2g}\uparrow \rightarrow e_g\uparrow$ ($G_2, \sim 1.8$ eV), $2p \rightarrow t_{2g}\downarrow$ ($G_3, \sim 4$ eV), $2p \rightarrow e_g\downarrow$ ($G_4, \sim 5.8$ eV), $e_g\uparrow \rightarrow$ La/Sr $5d$ ($G_5, \sim 9.7$ eV), $2p \rightarrow$ La/Sr $5d$ ($G_6, \sim 10.5$ eV), and $t_{2g}\uparrow \rightarrow$ La/Sr $5d$ (G_7,

TABLE I. Gaussian fitting parameters for the interband excitation $\sigma_{\text{inter}}(\omega)$ of $La_{0.825}Sr_{0.175}MnO_3$.

Oscillator	S_i (eV/Ω cm)	γ_i (eV)	ω_i (eV)
G_1	396	0.44	1.05
G_2	676	0.69	1.79
G_3	1744	0.48	4.10
G_4	4532	1.27	5.50
G_5	884	1.05	9.65
G_6	24457	2.29	10.39
G_7	4512	2.14	11.42

~ 11.5 eV). The energies are peak positions predicted from this diagram. The last three terms form the 10.5-eV peak, which originates mainly from the $2p \rightarrow$ La/Sr $5d$ CT excitation (G_6). The present diagram predicts two additional minor (hidden) peaks with initial states $e_g\uparrow$ and $t_{2g}\uparrow$ at frequency about 1 eV lower (G_5) and higher (G_7), respectively.

The most difficult task in this analysis is to estimate $\sigma_{\text{intra}}(\omega)$. We attempted to fit this term with a simple Drude formula $\sigma_0 \gamma^2/(\omega^2 + \gamma^2)$ or a simple Drude term plus an additional Gaussian (or Lorentzian), but the fitting is not good in each case. During our attempts, we found one formula, $\sigma_0 \gamma^\alpha/(\omega^\alpha + \gamma^\alpha)$ ($\alpha \sim 0.68$, $\gamma \sim 0.029$ eV), which can reproduce the low-energy part of $\sigma(\omega)$ accurately. This suggests that the Drude-like term is suitable for one-component analysis with a slowly decaying function. (Later, we discuss the possibility of *bad metallic nature* as an origin of this slowly decaying Drude-like term.) However, a $\omega^{-\alpha}$ function ($\alpha < 1$) decays so slowly that it has large spectral weight in the higher-energy region.

Next, we made the assumption that $\sigma_{\text{intra}}(\omega)$ has no weight above the reflectivity edge (~ 1.6 eV) and attempted to fit the higher-energy part of $\sigma(\omega)$ at 10 K with the seven Gaussians. As shown in Fig. 5, $\sigma(\omega)$ above 1.6 eV can be well represented by these seven Gaussians. Each term is represented by a dashed line. The fitting parameters are listed in Table I.[26] The following arguments/facts substantiate that the present diagram is, at least, not incompatible with the experiment: (i) The peak positions are, roughly speaking, coincident with the predictions. (ii) The hidden peaks G_1, G_2, and G_4 are indispensable for reproducing $\sigma(\omega)$. (iii) The lowest peak G_1 depends on the estimation of the Drude-like term to some extent, but the higher-lying five peaks ($i=3-7$) are not affected by variations in the estimate of the Drude-like term, and the position of the second peak is almost unchanged, though S_2 and γ_2 are slightly affected. This is reasonable because σ_{intra} and G_1 have no spectral weight in the higher-energy region. (iv) The present diagram also predicts that the additional exchange gap assigned as $t_{2g}\uparrow \rightarrow e_g\downarrow$ exists around 7 eV. However, even if this highest exchange gap exists, it has only small spectral weight compared with the total N_{eff}^*, as already mentioned.

In the present diagram, the charge carriers are $(1-x)$ *electrons*/Mn. This is consistent with the facts that the physical quantities reflecting the carrier density, such as the spectral weight of the Drude-like term[14] and the critical resistivity value for the Al-induced itinerancy-localization transition,[25] do not show remarkable x dependence. The Hall effect study[27] indicates that the carriers are about one *hole*/Mn and are nearly independent of x, which is consistent

with the present diagram except for the sign of the carrier. The difference of the sign is probably related to the electronic properties of this correlated-electron system, in which the simple free-carrier picture is not applicable. Otherwise, as is often argued, it is due to the carrier compensation effect, which is suggested by the band calculation.[28]

The present analysis enables us to extract a net contribution to $\sigma(\omega)$ from the conducting carriers, $\sigma_{intra}(\omega) \equiv \sigma(\omega) - \sigma_{inter}(\omega)$ (inset of Fig. 5). It can also refine the estimation of Drude weight, which is estimated to be 0.23/Mn at 10 K, by integrating σ_{intra}. This is consistent with the recent precise optical absorption experiment.[29] The intraband charge dynamics is, on the other hand, characterized by the ''coherent-incoherent'' crossover.[16,17] In the higher-T region below T_C, a Drude-like term is absent and, instead, a broad peak at finite frequency is dominant in $\sigma(\omega)$, although the dc resistivity $\rho(T)$ is metallic in character ($d\rho/dT > 0$). A Drude-like term is present only at sufficiently low T (or low ρ). These features may be interpreted as the optical response of a *bad metal*.[30,31] The recent resistivity study suggests that LSMO can be classified as a bad metal.[25] The crossover in $\sigma(\omega)$ mentioned above occurs when the mean free path of the conducting carrier reaches the Fermi wavelength. A similar crossover is also observed for the typical bad metal SrRuO$_3$.[32] In this scenario, the slowly decaying Drude-like term in the ''low-T coherent'' region is a possible indication (or reminiscent) of diffusive conduction, which yields the broad peak of $\sigma(\omega)$ in the ''high-T incoherent'' region.

In summary, the split of the exchange-gap excitation in $\sigma(\omega)$ indicates that the t_{2g} orbitals participate in the reconstruction of the optical excitation caused by spin polarization in LSMO. Based on the present result, we propose a band diagram for this compound, which is helpful for improving our understanding of its electronic structure as well as the charge dynamics of the conducting carriers in the doped ferromagnetic-metallic phase. The dynamics of the carriers is discussed in terms of being a bad metal.

*Electronic address: k46291a@nucc.cc.nagoya-u.ac.jp

[1] For a review, see T. A. Kaplan and S. D. Mahanti, *Physics of Manganites* (Plenum, New York, 1999).

[2] N. Furukawa, J. Phys. Soc. Jpn. **64**, 3164 (1995); see also Ref. 1.

[3] A. J. Millis, R. Mueller, and Boris I. Shraiman, Phys. Rev. B **54**, 5405 (1996).

[4] S. Ishihara, M. Yamanaka, and N. Nagaosa, Phys. Rev. B **56**, 686 (1997).

[5] P. E. de Brito and H. Shiba, Phys. Rev. B **57**, 1539 (1998).

[6] S. Yunoki, A. Moreo, and E. Dagotto, Phys. Rev. Lett. **81**, 5612 (1998).

[7] A. S. Alexandrov and A. M. Bratkovsky, Phys. Rev. Lett. **82**, 141 (1999).

[8] P. Horsch, J. Jaklič, and F. Mack, Phys. Rev. B **59**, 6217 (1999).

[9] H. Nakano, Y. Motome, and M. Imada, J. Phys. Soc. Jpn. **69**, 1282 (2000).

[10] K. Held and D. Vollhardt, Phys. Rev. Lett. **84**, 5168 (2000).

[11] Y. Okimoto *et al.*, Phys. Rev. B **55**, 4206 (1997).

[12] Y. Moritomo *et al.*, Phys. Rev. B **56**, 5088 (1997).

[13] M. Quijada *et al.*, Phys. Rev. B **58**, 16 093 (1998).

[14] K. Takenaka *et al.*, J. Phys. Soc. Jpn. **68**, 1828 (1999).

[15] H. J. Lee *et al.*, Phys. Rev. B **60**, 5251 (1999).

[16] E. Saitoh *et al.*, Phys. Rev. B **60**, 10 362 (1999).

[17] K. Takenaka, Y. Sawaki, and S. Sugai, Phys. Rev. B **60**, 13 011 (1999).

[18] A. Urushibara *et al.*, Phys. Rev. B **51**, 14 103 (1995).

[19] For nickelates, see, T. Katsufuji *et al.*, Phys. Rev. B **54**, R14 230 (1996).

[20] The spectral weight of the 3.2-eV band depends on the lower cutoff energy in the integration to some extent, but the relation between the weight and $M(T)$ does not.

[21] M. Abbate *et al.*, Phys. Rev. B **46**, 4511 (1992).

[22] S. Tajima *et al.*, J. Opt. Soc. Am. B **6**, 475 (1989).

[23] J. H. Jung *et al.*, Phys. Rev. B **55**, 15 489 (1997).

[24] T. Arima and Y. Tokura, J. Phys. Soc. Jpn. **64**, 2488 (1995).

[25] Y. Sawaki, K. Takenaka, A. Osuka, R. Shiozaki, and S. Sugai, Phys. Rev. B **61**, 11 588 (2000).

[26] The optical excitations depend on the d-p hybridization. Therefore, the d-d excitations become active and S_i does not necessarily reflect the carrier number (capacity).

[27] A. Asamitsu and Y. Tokura, Phys. Rev. B **58**, 47 (1998).

[28] Warren E. Pickett and David J. Singh, Phys. Rev. B **53**, 1146 (1996).

[29] J. R. Simpson *et al.*, Phys. Rev. B **60**, R16 263 (1999).

[30] V. J. Emery and S. A. Kivelson, Phys. Rev. Lett. **74**, 3253 (1995); P. B. Allen *et al.*, Phys. Rev. B **53**, 4393 (1996).

[31] The present argument is one of the possible interpretations, and hence does not exclude other possibilities, for example, the two-component picture, in which the slowly decaying Drude-like term consists of a simple Drude term and an incoherent broad peak.

[32] P. Kostic *et al.*, Phys. Rev. Lett. **81**, 2498 (1998).